We are IntechOpen,
the world's leading publisher of
Open Access books
Built by scientists, for scientists

4,800
Open access books available

122,000
International authors and editors

135M
Downloads

Our authors are among the

154
Countries delivered to

TOP 1%
most cited scientists

12.2%
Contributors from top 500 universities

CLARIVATE ANALYTICS

BOOK CITATION INDEX

INDEXED

WEB OF SCIENCE™

Selection of our books indexed in the Book Citation Index
in Web of Science™ Core Collection (BKCI)

Interested in publishing with us?
Contact book.department@intechopen.com

Numbers displayed above are based on latest data collected.
For more information visit www.intechopen.com

Study of a New Type High Strength Ni-Based Superalloy DZ468 with Good Hot Corrosion Resistance

Enze Liu and Zhi Zheng
Institute of Metal Research, Chinese Academy of Sciences
China

1. Introduction

There is a great demand for advanced nickel-based superalloys, mainly for the application to industrial gas turbine blades. They should possess an excellent combination of hot corrosion resistance and high temperature strength. Despite the recent innovation of coating technology, hot corrosion resistance is still important for industrial turbines which are for a long term service. An increasing demand for the higher efficiency of gas turbines leads to the necessity of rising their operating temperatures and stresses, which requires a continued development of high strength superalloys for gas turbine components. Hot corrosion resistance is also important for industrial turbines, which are used for longer term than jet engines. Furthermore, oxidation resistance needs to be improved because of the general increase in the inlet-gas temperature of turbines [1, 2]. In order to improve high temperature strength, it is necessary to add Al, Ti, Nb, Ta, W, Mo, and so on. In order to gain good hot corrosion resistance property, Cr is indispensable alloying element in superalloys for maintaining hot corrosion resistance [3, 4]. However, the improvement in one property by adding one or more elements into the alloy may be accompanied by the deterioration of another property [5]. For example, the addition of Re improves both high-temperature creep strength and the hot corrosion resistance [6, 7]. However, increasing in the Re content in SC superalloys has the propensity to precipitate Re-rich topologically closed packed (TCP) phases which is known to reduce creep rupture strength [8, 9, 10].DZ125 alloy is one of using operating turbine blade with excellent mechanic property. IN738 alloy with excellent hot corrosion resistance was broadly using to produce industrial gas turbine blades. In this paper, we hope research a new alloy with the same mechanical property as that of DZ125 alloy and the same hot corrosion resistance as that of IN738 alloy on the basis of good phase stability. Based on DZ125 and IN738 alloys, a new alloy namely DZ468 was developed by institute of metal research, Chinese academy sciences. DZ468 show good mechanics properties, good environment properties and good phase stability.

2. Experiments and results

The DZ468 superalloy is a second-generation nickel-based directed solidified alloy developed by Institute of Metal Research; Chinese Academy of Sciences (IMR, CAS) based

on DZ125 and IN738 alloys. Table 1 shows the compositions of DZ125, IN738 and DZ468 alloys. The alloy was melted in VZM-25F vacuum induction furnace. The directionally solidified specimens were made by the process of high rate solidification in ZGD2 vacuum induction directional solidification furnace. The temperature gradient was 80°C/cm and the withdrawal rate was 6 mm/min. The procedure of heat treatment was following: 1240°C/0.5 h +1260°C/0.5h +1280°C/2 h,AC+1120°C/4h, FC to 1080°C with 1h+1080°C /4h,AC+900°C /4h,AC (AC: air cooling, FC: fuel cooling).

Alloy	C	Cr	Mo	W	Co	Al	Ta	Ti	Re	Nb	Zr	Hf	B	Ni
DZ468	0.05	12	1	5	8.5	5.5	5	0.5	2.0	–	–	–	0.01	Bal.
IN738	0.05	16	1.8	2.6	8.5	3.5	1.8	3.2	–	0.8	0.1	–	0.01	Bal.
DZ125	0.08	9	2	7	10	5.2	3.8	1.0	–	–	–	1.5	0.015	Bal.

Table 1. Nominal composition of test alloys (mass fraction, %)

2.1 Microstructure

The microstructure of cast and heat treatment of DZ468 alloy were observed by scanning electron microscope(SEM) and optical microscope(OM).The specimens used for SEM were electrolyzed in a solution of 5ml HNO_3+10ml HCl+5ml H_2SO_4+100ml H_2O with a voltage of 7V. Rectangular specimens with dimensions of 10mm×10mm×8mm were cut by the electrical-discharge method. As shown in the Fig.1a, the microstructure of as-cast alloy are composed of γ, γ′, carbides of MC type, (γ+γ′) eutectic and a little boride at the edge of (γ+γ′) eutectic. Fig.1b shows the size of γ′ phase is large and the shape is roughly cubic. Most γ′ phase particles show cube shape, but some reveal exaggerated octagonal form.
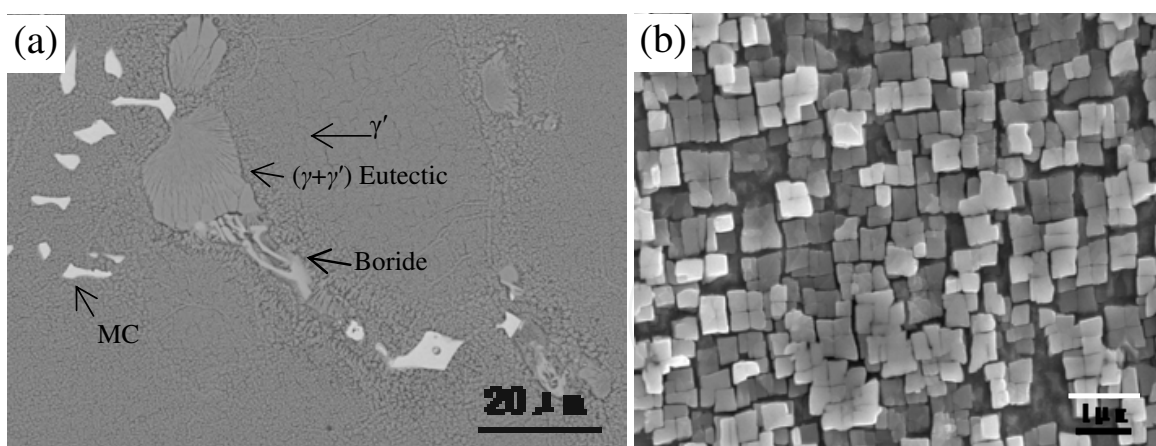

Fig. 1. Microstructure of cast DZ468 alloy (a) OM, (b) SEM

Microstructure of DZ468 alloy after heat treatment shows in the Fig.2a. After heat treatment, the microstructure of DZ468 alloy is composed of γ, γ′ and carbides. The carbides are mainly MC and $M_{23}C_6$. There is no finding (γ+γ′) eutectic and boride in the Fig.2a. After heated, γ′ phase show good cubic shape and the variant size of γ′ on inter–dendrite region and dendrite core is rather small as shown in the Fig.2b and Fig.2c. The microstructure of DZ468 alloy after aging at 900°C for 1000h was shown in the Fig.3. After prolong exposure, Coarsening of the γ′ was observed and there is no finding TCP phase in the Fig.3. The types

of carbide only are MC and $M_{23}C_6$ and there is a very small amount of acicular $M_{23}C_6$. It can be seen from Fig.2 and Fig.3 that DZ468 alloy displays excellent phase stability and uniform microstructure.
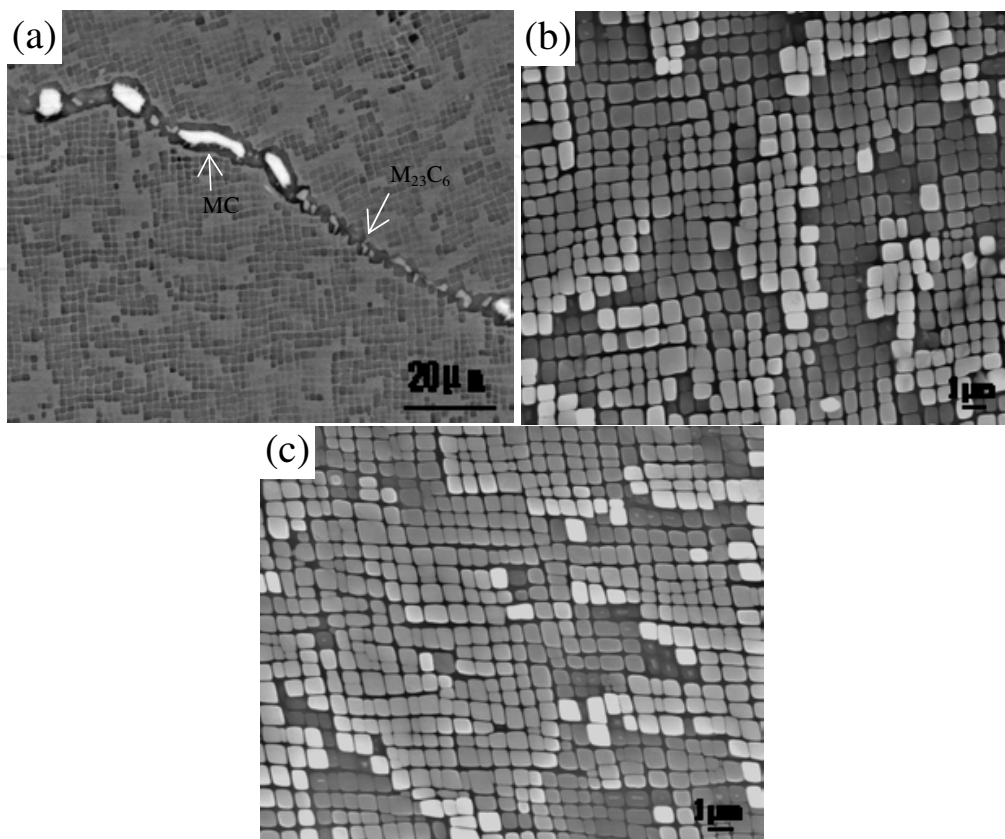

Fig. 2. Microstructure of DZ468 alloy after heat treatment (a) in the grain boundary (b) γ′ on inter-dendrite region, (c) γ′ on dendrite core
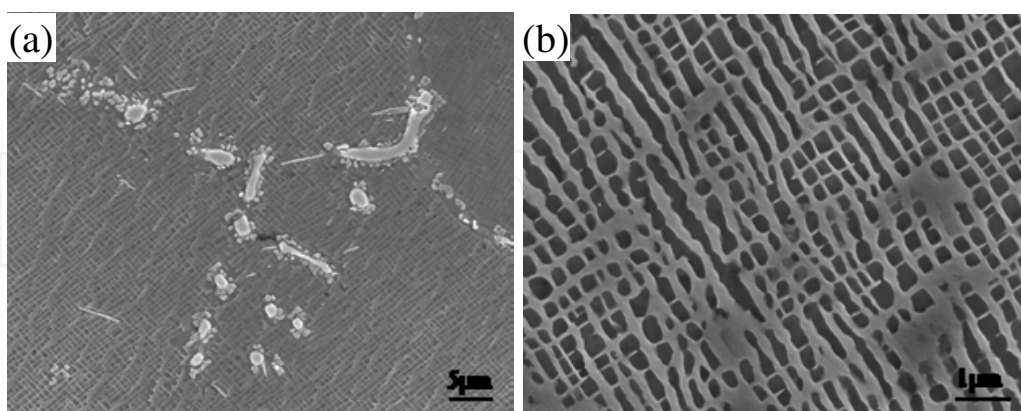

Fig. 3. Microstructure of DZ468 alloy after prolong exposure at 900℃ for 1000h (a) in the grain boundary (b) morphologies of γ′

2.2 Tensile properties

The tensile tests were performed at different temperatures from room temperature to 1000℃ a DCX-25T type universal test machine at a constant strain rate of $10^{-4}s^{-1}$. As shown in Fig.4,

the change of tensile strength and yield strength of three alloys is similar. When temperature is lower than 760ºC, the tensile strength(σ_b) and yield strength($\sigma_{0.2}$) of three alloys change slightly with increasing temperature. When the temperature is more than 760ºC, the tensile strength and yield strength decrease sharply. The tensile strength and yield strength of DZ468 alloy is nearly the same as that of DZ125 alloy in the same condition, but its more than that of IN738 alloy.

The elongation (δ) and reduction of area (φ) are not without significant change from room temperature to 760ºC in three alloys. When the temperature is more than 760ºC, δ and φ quickly increase. As a whole, Ductility of DZ125 alloy displays better than that of DZ468 alloy in lower temperature, but difference of ductility between DZ125 alloy and DZ468 alloy is slightly in higher temperature.
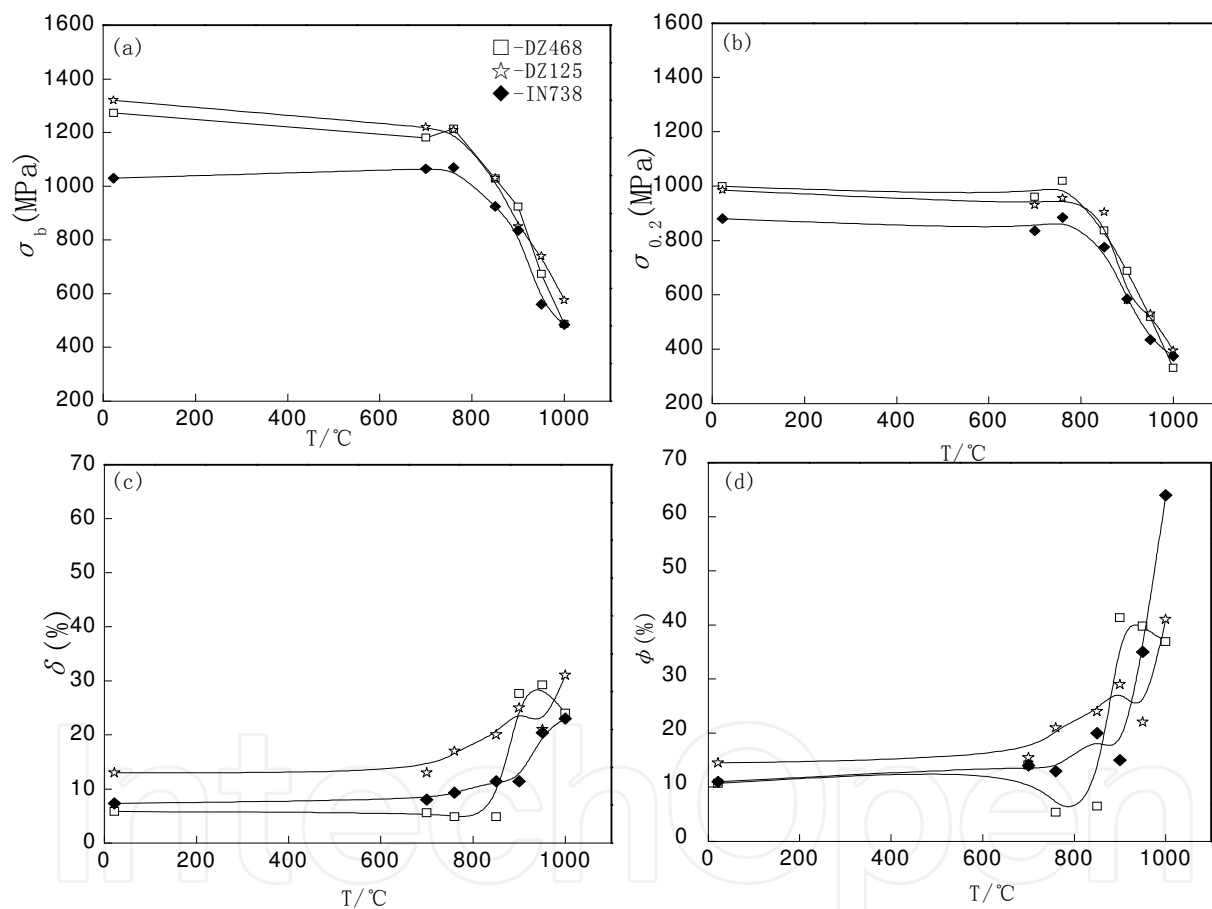
Fig. 4. Tensile properties of DZ468, DZ125 and IN738 alloys (a) the tensile strength, (b) the yield strength, (c) the elongation, (d) the reduction of area

2.3 The rupture properties

Constant load creep and rupture tests in air were carried out at different temperatures for specimens sampled from bars with normal heat treatments. Fig .5 shows the relationship between stress and time to rupture for specimens. The general trend of the rupture data was that the rupture life increased with decreasing test stress and test temperature, as is normally observed from other alloys. Fig.6 shows Larson- Miller curves of three alloys. It

can be seen from Fig.6 the creep rupture life of DZ468 alloy is similar that of DZ125 alloy and observably more than that of IN738 alloy.
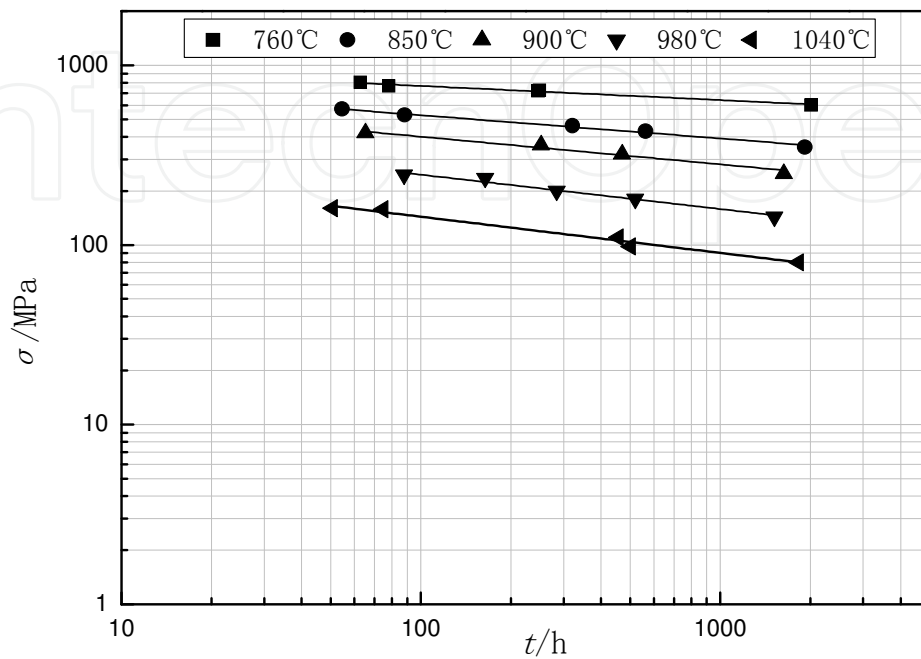

Fig. 5. Stress versus time to rupture in air for DZ468 alloy with different temperature and stress
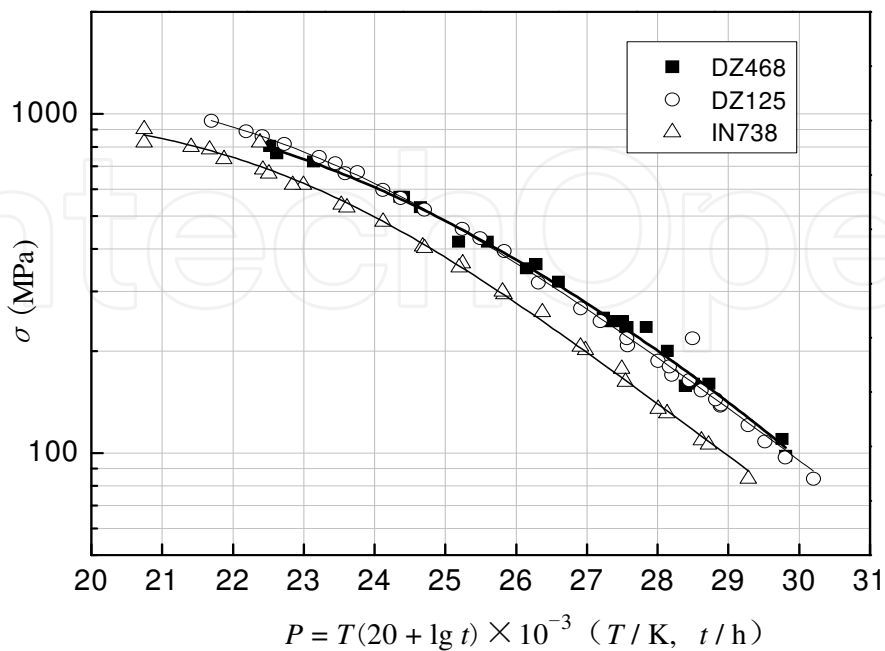

$$P = T(20 + \lg t) \times 10^{-3} \ (T/\mathrm{K}, \ t/\mathrm{h})$$

Fig. 6. Larson- Miller curves of DZ468, DZ125 and IN738 alloys

From Table 1, it can be seen the sum of Al, Ti and Ta respectively is 14.2 %(atom fraction) in DZ468 and13.8 %(atom fraction) DZ125 alloy. Hence, the γ′ volume fraction of DZ468 and DZ125 is equivalent. In the DZ125 and DZ468 alloys, the total content of strengthening γ phase element W, Mo, Re is almost equivalent. Hence, creep rupture life of DZ468 alloy is similar to that of DZ125 alloy. It can be seen from Fig.7 the creep rupture life of DZ468 alloy to that of DZ125 alloy.

2.4 The creep properties

The creep curves of strain (ε) versus time (t) at different temperatures and stress levels are shown in three figures(fig.7, fig.8 and fig.9). It is indicated that the shape of the creep curve exhibits strong temperature and stress dependence, and the strain rate during steady-state creep is enhanced and creep lifetimes are obviously shortened with the increase of the applied stresses. The observed creep curves are similar and show a respective course at the same testing temperature. The creep curves show an obvious primary creep stage followed by an extended steady-state creep stage and then an accelerating creep stage leading to failure at 760℃ (Fig.7). The 850℃ creep curves demonstrate a very short primary stage, and a longer accelerating creep stage without steady-state creep stage(Fig. 8).It can be seen from fig.7, fig.8 and fig.9, with the increasing of test stress, the creep rate is obviously increasing. Table.2 and table.3 show the creep strength of DZ468 and DZ125 alloys. At the same condition of temperature, the creep strength of DZ468 is lower than that of DZ125 alloy.
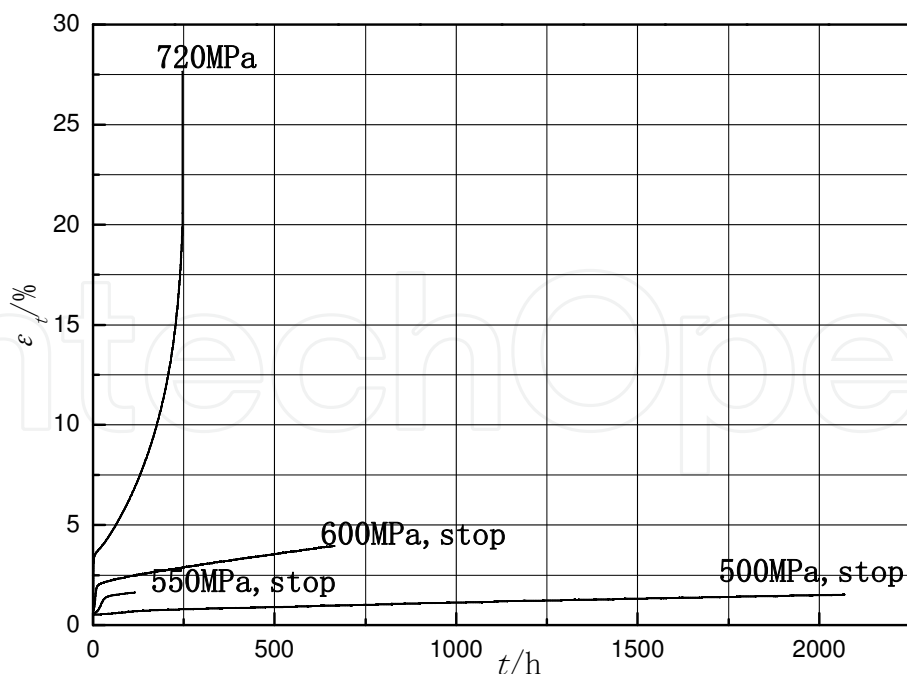

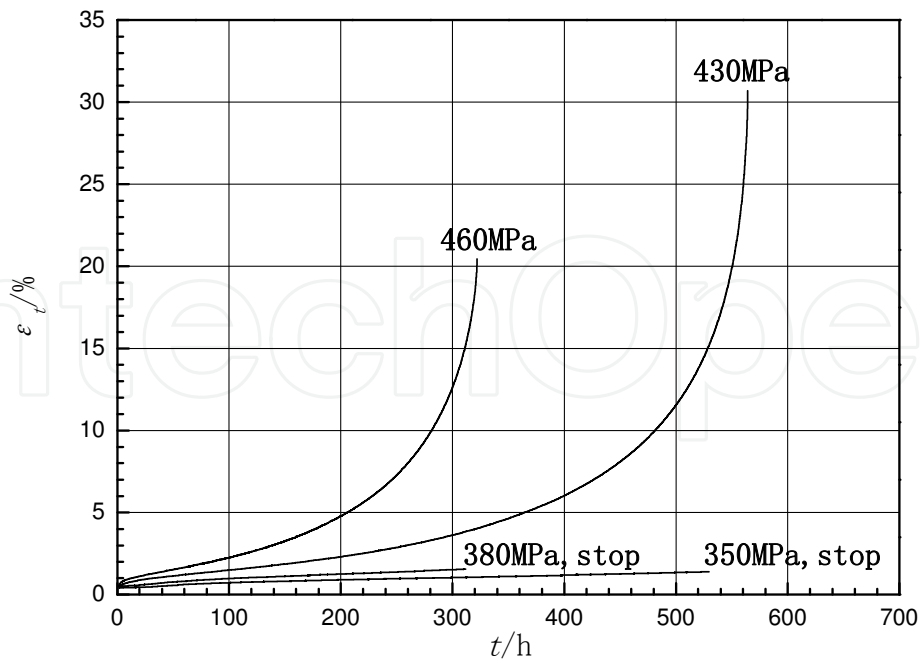Fig. 7. Creep curves of DZ468 alloy at 760ºC with different stress

Fig. 8. Creep curves of DZ468 alloy at 980ºC with different stress
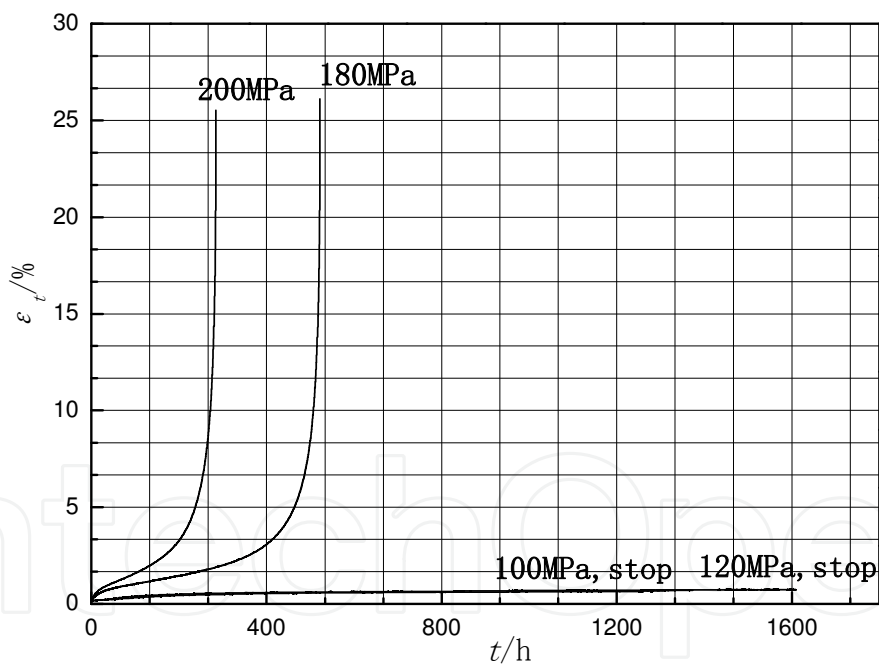

Fig. 9. Creep curves of DZ468 alloy at 850ºC with different stress

T/℃	$\sigma_{0.1/100h}$/MPa	$\sigma_{0.2/100h}$/MPa	$\sigma_{0.5/100h}$/MPa
760	530	545	591
850	337	343	405
980	126	140	168

Table 2. The creep strength of DZ468 alloy with different plasticity strain at different temperature

T/℃	$\sigma_{0.1/100h}$/MPa	$\sigma_{0.2/100h}$/MPa	$\sigma_{0.5/100h}$/MPa
760	550	595	620
850	340	380	420
980	170	190	230

Table 3. The creep strength of DZ125 alloy with different plasticity strain at different temperature

2.5 High cycle fatigue

The airfoil sections of turbine blades in aircraft engines are subjected to very high temperatures, high stresses, and aggressive environments. These factors can lead to fatigue behavior that is quite complex, and dependent on stress level (both alternating and mean) and creep and environmental effects. High-cycle fatigue (HCF) tests were performed using smooth round-bar specimens on a high frequency MTS machine. The average test frequency is 120HZ and the R-ratio (R =minimum/maximum stress) is -1. The temperature is 760℃ and 900℃. The results, plotted as test life in cycles to failure vs. stress amplitude, are shown in Fig.10. The general trend of the S-N data was that the fatigue life increased with decreasing maximum stress level, as is normally observed from fig.10. It can also be noticed that the fatigue limits of DZ468 alloy at 760℃ was higher than that at 900℃.
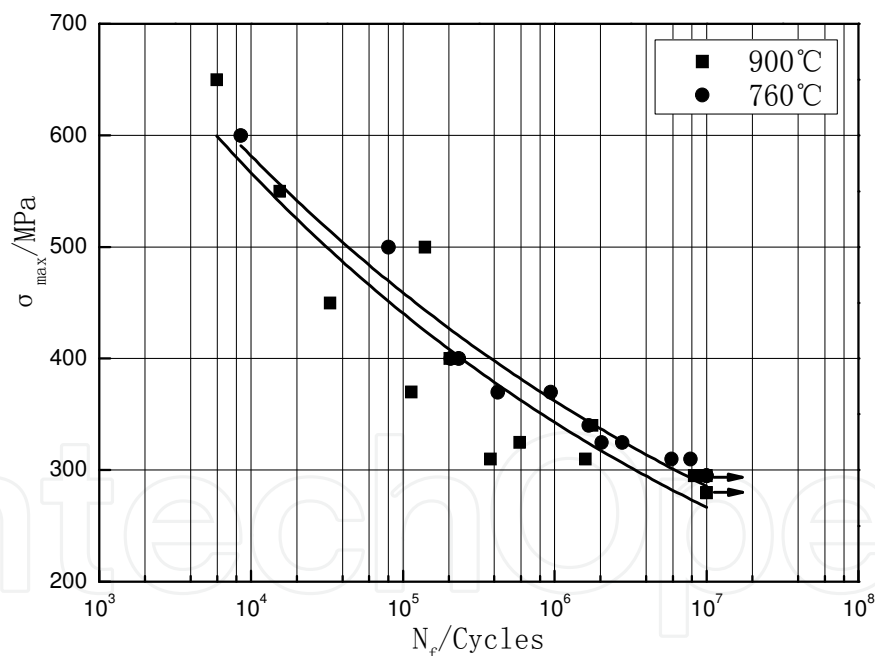

Fig. 10. The HCF S-N curves of DZ468 alloy at 760℃ and 900℃, the average test frequency is 120HZ and the R-ratio is -1.

2.6 Low cycle fatigue

The high temperature low cycle fatigue (LCF) failure is the major factor affecting the service life of the turbine blades. The type of fatigue tests and the experimental conditions were chosen in order to simulate the loading conditions of turbine blades knowing that these conditions are much more complex. LCF specimens were machined from solution treated

bars with 15mm in diameter and 25mm in gage length. Before testing, non-destructive evaluation was used to check out the casting pores in specimens. A servo hydraulic testing machine was used to perform the fatigue tests at 800℃ in air. The total axial strain was measured and controlled by an extensometer mounted upon the ledges of specimens. The total strain range ($\Delta\varepsilon_t$) varied from ±0.15 to ±0.6% with a fully reversed strain-controlled push–pull mode, i.e., $R\varepsilon=\varepsilon min/\varepsilon max=-1$. The strain rate was $4\times10^{-3}s^{-1}$, applied in a triangular waveform with a frequency f=0.35 Hz. The temperature fluctuation over the gage length area was maintained within ±2 ºC. Three specimens were prepared for each strain range at least. From the viewpoint of engineering applications, an important measure of a material LCF performance is the fatigue life as a function of total strain range, which is presented in Fig. 11 that shows the relationship curves of the total strain range versus number of cycles to failure. The fatigue life shows a monotonic decrease with increasing total strain range from 800℃. It can be seen from fig.11, the fatigue life of DZ125 is slightly longer than that DZ468 at the same total strain range.
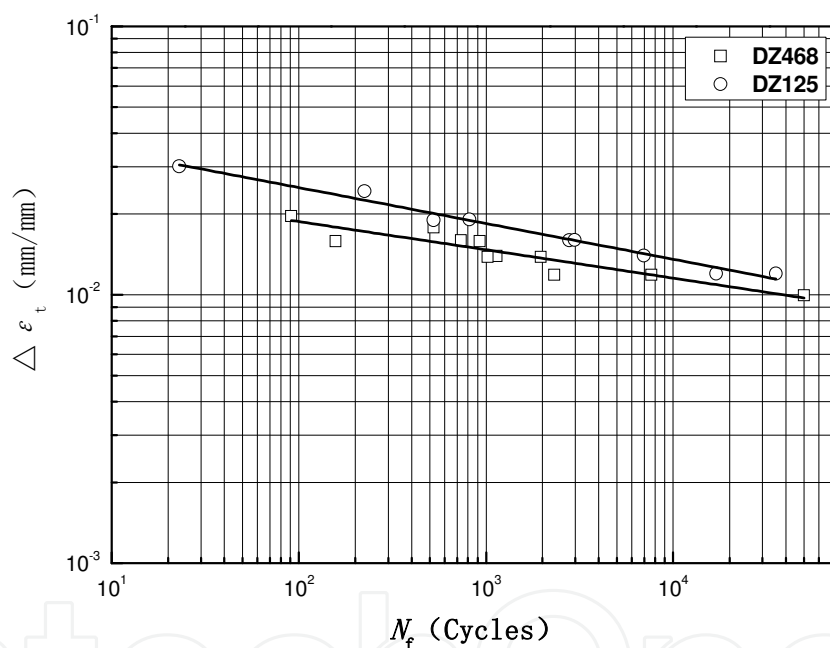

Fig. 11. Fatigue life of DZ468 and DZ125 alloys as a function of total strain range at 800ºC

2.7 Hot corrosion resistance

The hot corrosion tests were conducted at 900ºC. The surfaces were polished down to 1000-grit alumina paper. A mixture of 75% Na_2SO_4+25% (mass fraction) NaCl was used for hot corrosion experiment. The specimens and mixed salts contained in an Al_2O_3 crucible were placed in a muffle furnace after the furnace reached the desired temperature.

Fig.12 shows hot corrosion dynamics curves of DZ125, IN738 and DZ468 alloys. Both the DZ125 and IN738 alloys exhibit larger depth changes than DZ468 alloy. The absolute value of the depth change is the largest in the DZ125 alloy and the smallest in the DZ468 alloy. The element, Cr is well known to play an essential role in hot corrosion resistance, since it promotes the formation of a protective Cr_2O_3 scale [11]. Although the DZ468 alloy contains

the middle Cr content among three experimental alloys, it shows the best hot corrosion resistance. This is due to Re content (2 Mass fraction %) in DZ468 alloy. As already reported, Re is effective in improving hot corrosion resistance as well as creep rupture strength [11, 12, 13]. Furthermore, DZ468 is a kind of low segregation alloy which has own uniform microstructure and chemical composition.
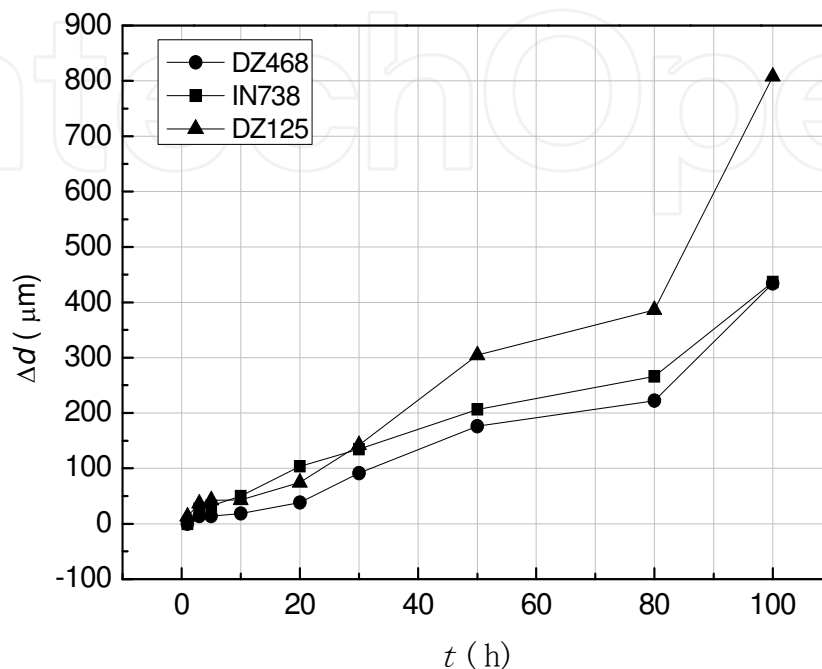

Fig. 12. Hot corrosion dynamics curves of DZ468, DZ125 and IN738 alloys in mixture of 75% Na_2SO_4+25% (mass fraction) NaCl at 900℃

2.8 Physics properties

The density of DZ468 alloy is about to 8.45g/cm^3. Fig.13 shows the mean linear thermal expansion coefficients (CTEs) of DZ468 and DZ125 alloy. It can be seen from fig.13, the l CTEs of DZ125 are larger than that of DZ468 alloy. Fig.14 shows the thermal conductivity of DZ468 and DZ125 alloys at different temperature. It can be seen from fig.14, when the temperature is more than 900℃, the thermal conductivity of DZ468 is higher than that of DZ125 alloy. The thermal conductivity of DZ468 alloy shows a monotonic increase with increasing temperature. Table.4 shows the Young's elastic modulus (E) of DZ468 and DZ125 alloy. The Young's elastic modulus (E) of DZ468 is decreasing with the increasing of test temperature. It is similar to the Young's elastic modulus DZ468 and that of DZ125.

T/℃	20	100	200	300	400	500	600	700	800	900	1000	1100
DZ468 /GPa	132.09	126.66	123.37	120.38	116.63	111.57	106.53	100.52	95.49	88.67	81.15	70.16
DZ125 /GPa	131.73	126.36	123.52	120.54	116.51	111.31	106.47	100.61	95.36	88.77	81.50	70.08

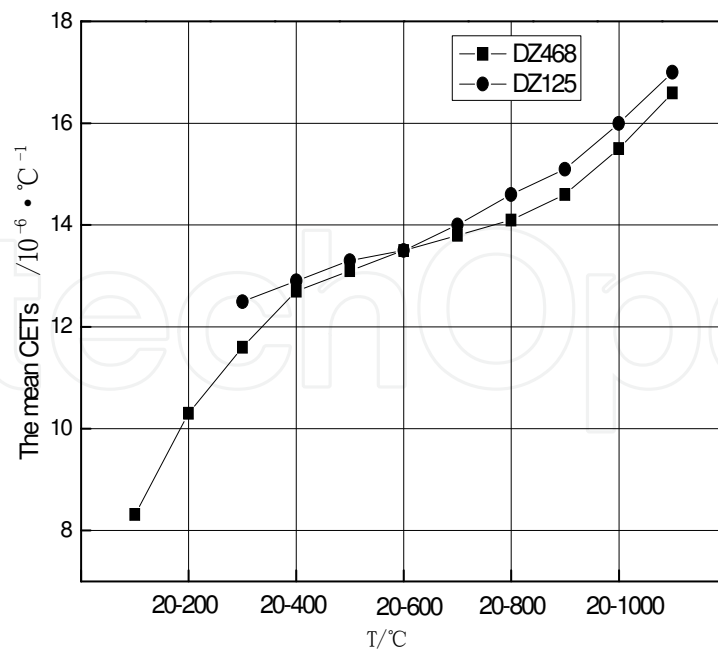Table 4. The Young's elastic modulus of DZ468 and DZ125 alloys

Fig. 13. The mean Linear Thermal Expansion Coefficient (CETS) of DZ468 and DZ125 alloys at different temperature interval
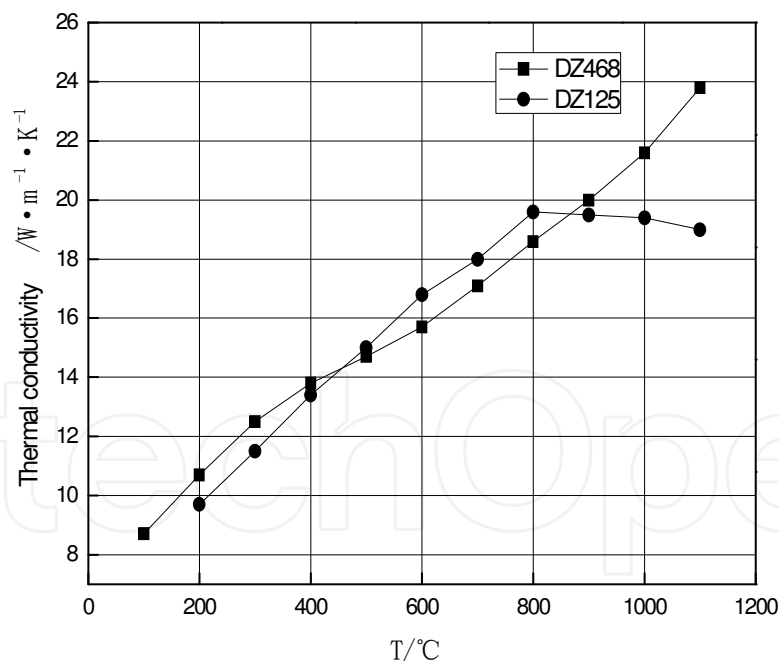

Fig. 14. The thermal conductivity of DZ468 and DZ125 alloys at different temperature

3. Conclusion

A new-typed directional solidification nickel-base superalloy that is named DZ468 was designed by low segregation technology. Microstructures of DZ468 as cast alloy are composed of γ, γ′,(γ+γ′) eutectics, MC type carbides and a few borides. After heat treatment,

the microstructures of DZ468 alloy are composed of γ, γ′, MC and $M_{23}C_6$. DZ468 has excellent phase stability, good mechanics properties, physics properties and environment properties.

4. Acknowledgment

5. References

[1] Y.Murata, S. Miyazaki, et al., in: *Superalloys 1996*, edited by R. D. Kissinger, D. J, Deye, et al.,TMS (1996).

[2] Duhl David N, Chen Otis Y, GB Patent 2, 153, 848. (1985)

[3] Yamazaki Michio, Harada Hiroshi, U.S. Patent 4, 205, 985. (1980)

[4] Duhl, David N., Chen, Otis Y., U.S. Patent 4,597, 809. (1986)

[5] Sato Koji, Ohno Takehiro, Yasuda Ken, et al., U.S. Patent 5, 916, 382. (1999)

[6] Cetel Alan D., U.S. Patent 111,138. (2003)

[7] Cetel Alan D., Shah Dilip M., U.S. Patent 200,549. (2004)

[8] Sato Masahiro, Takenaka Tsuyoshi, et al., U.S. Patent 47,110(2010)

[9] T. Kobayashi, M. Sato, et al.in:*Superalloys 2000*,edited by T.M. Pollock, R.D. Kissinger, et al., TMS, (2000)

[10] Y. Murata, M. Morinaga, et al.: ISIJ International, Vol. 43(2003), p.1244

[11] K. Matsugi, Y. Murata, et al, in: *Superalloys 1992*, edited by S. D. Antolovich, R.D. Kissinger, et al., TMS, Warrendale, PA, (1992)

[12] K. Matsugi, M. Kawakami, et al.: Tetsu-to-Hagané, Vol.78 (1992), p.821

[13] T. Hino, Y. Yoshioka, K. Nagata, et al.in: *Materials for Adv. Power Eng.1998,* edited by J.Lecomte-Beckers et al., Forschungszentrum Julich Publishers, Julich, (1998)
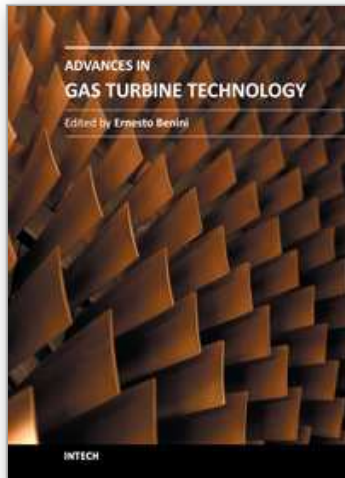
Advances in Gas Turbine Technology

Edited by Dr. Ernesto Benini

Gas turbine engines will still represent a key technology in the next 20-year energy scenarios, either in stand-alone applications or in combination with other power generation equipment. This book intends in fact to provide an updated picture as well as a perspective vision of some of the major improvements that characterize the gas turbine technology in different applications, from marine and aircraft propulsion to industrial and stationary power generation. Therefore, the target audience for it involves design, analyst, materials and maintenance engineers. Also manufacturers, researchers and scientists will benefit from the timely and accurate information provided in this volume. The book is organized into five main sections including 21 chapters overall: (I) Aero and Marine Gas Turbines, (II) Gas Turbine Systems, (III) Heat Transfer, (IV) Combustion and (V) Materials and Fabrication.

How to reference

In order to correctly reference this scholarly work, feel free to copy and paste the following:

INTECH
open science | open minds